J. Basic. Appl. Sci. Res., 4(2)236-255, 2014

ISSN 2090-4304
Journal of Basic and Applied Scientific Research
www.textroad.com

Efficient Detection of Malignant Tumor by Eliminating Artifacts in Electroencephalogram Using Ica

A. Rashid[1], I. M Qureshi[2], A. Naveed Malik, T. A Cheema

[1]A P EE Department, Air University Islamabad, Pakistan
[2]Professor, EE Department, Air University, Islamabad, Pakistan
[3,4]Professor, EE Department, Isra University Islamabad, Pakistan

Received: November 20 2013
Accepted: December 16 2013

ABSTRACT

A new scheme introduced in this work focuses on the solution of two problems. One is Efficient Extraction of artifacts present in Electro-Encephalo-Gram(EEG) signal. Second is how to detect the features of Malignant Tumors in suspicious regions, specifically when they have a very low contrast to their background, using EEG signals supporting with fMRI images. This work provides efficient detection of malignant brain tumor followed by the description of EEG and fMRI signals/images and their clinical utilities for differential diagnosis, tumor grading and response to treatment assessment. The EEG signal taken from the skin of the patient body is affected by Lung noise, baseline noise, power line noise and muscle noise. The noises and the artifacts which highly contaminate EEG signal arrive both from subject and from EEG machine interferences. For efficient Malignant brain tumor detection it is necessary to extract useful EEG features buried in the wide band of noise. For efficient Malignant brain tumor detection the fast ICA(FASTICA)filter is being proposed in this research.

KEYWORDS: EEG, fMRI, Baseline, Kalman, Detection, Independent Component Analysis, FASTICA.

1. INTRODUCTION

The EEG and ECG are the basic tools of studying brain and heart activities respectively. The study of these instruments with reference to brain tumor and severe heart attack is of vital importance. The Loose sensor contacts, breathing, patient body and eye movements are the main source of baseline noise. Many researchers have applied different algorithms to remove these artifacts Important of these are Kalman filter, Cubic spline, or Moving average. The Electrical potential variations at multiple locations over the scalp are recorded by EEG in the form of a signal. The most widespread artifact in EEG signal is the Electrooculogram (EOG). EOG is produced by eye movement or by eye blinks. The amplitude of EOG signal is comparatively high even ten times larger than average cortical signal [4]. Because of this high magnitude, the signals recorded over occipital areas(eyes and scalp tissues) are highly contaminated with artifacts. The eye blink artifacts can efficiently be eliminated while keeping those signals safe representing brain activity.

The EEG signals carry significant information. The EEG signal obtained from electrodes placed at the scalp cary large amount of electrical energy[3]. The potentials collected from independent neurons inside the brain carry great deal of information for researchers. Placing the EEG electrodes inside the human head comparatively give more useful information. The electrical activity produced by cerebral cortex nerve cells carrying useful information about patient in the form of EEG signals is intensively used for clinical assessment of brain activities and functions. It is also widely employed for the identification of epileptic form discharges in the Electro-Encephalo-Gram. This research work shows an efficient approach for early brain tumor detection by removing artifacts in EEG using Independent Component Analysis (ICA) technique. Independent Component Analysis was proposed by Camon in 1994 in the context of solving blind source separation (BSS) problems. Now a days ICA has emerged as a novel tool for eliminating artifacts from EEG and ECG data for efficient detection of tumor. ICA separate a set of mixed signals without knowing anything about the number of original signals how they are mixed. ICA separates a set of data in to its statistically independent components. These components can then be studied and those identified as artifacts can be eliminated. In this research we have used ICA to eliminate artifacts of EEG so that detection of Malignant tumor can be performed efficiently.

1.1 Brain Tumor

An incongruous and anomalous magnification of sells inside the skull of the brain become a source of brain tumor. This Tumor can be a cancerous or non-cancerous. Tumor that gets its roots inside the brain tissues is called primary tumor of the brain. These primary tumors are differentiated considering the type of the cells and to the place of the brain from where they are growing. Tumor grows because of the uncontrolled and abnormal cell division. Cell division took place in glial cells, neurons, oligodendrocytes, astrocytes, ependymal cells, blood vessels and lymphatic tissues. The tumor may also commence from the myelin-producing schwann cells called cranial nerves. The abnormal growth may appear in brain envelopes such as meninges, skull. Pineal gland and pituitary may also observe abnormal cell division. The tumor may spread from the cancers located in other organs such as metastatic tumors may also spread tumor [4]

[*]**Corresponding Author:** A. RASHID, A P EE Department, Air University Islamabad, Pakistan

1.2 Research Objective

Efficient method has been proposed for removing artifacts from EEG signals which in turn detect brain tumor efficiently. EEG records carry information about abnormalities and responses of brain of tumor patient. Various artifacts and noises are highly contaminating EEG signals. These artifacts are caused by factors like, line interference, subject movements, loose transducer contacts with human body, muscle activity, heart beat and field around the eyes(EOG). To eliminate the artifacts from EEG signals we have employed Analogue filtering method. In this method the reference signal EOG is used as input and EOG artifacts of EEG and ECG base line noise are subtracted. The analogue filtering is being performed by ICA technique. Removing these artifacts in EEG signals using ICA or FASTICA algorithm will significantly increase the chances of early tumor detection in brain.

2. PROBLEM FORMULATION & PROPOSED SOLUTION

The following assumptions for the ICA ensure that ICA model estimates the independent components meaningfully.

1. The independent components are statically independent and the mixing must be linear.
2. Among the latent variables there must not be more than one Gaussian signal and the cumulative density function of latent variables should not be much different from *logistic sigmoid.*
3. The number of the latent variables *n* are less than or equal than the number of the observed variables *m (*i.e *m≥n.).* Many efforts have been made to solve this problem but no concrete solution yet. There appears a redundancy in the mixed signals when *m>n.* when *m=n* the ICA works ideally.
4. The mixing matrix is of full column rank, which means that the rows of the mixing matrix are linearly independent. If the mixing matrix is not of full rank then the mixed signals will be linear multiples of one another.
5. Mixing matrix has negligible propagation delay.

The first assumption is of much significance while the other assumptions ensure that the estimated independent components are unique.

Consider a mixture of N sources $s_1(t),s_2(t),\ldots\ldots,s_N(t)$. Which are unknown but are assumed to be statistically independent from the observation of the *M* signals $x_1(t),x_2(t)\ldots\ldots\ldots,x_M(t)$. These signals result from a mixture of underlying sources. ICA needs at least as many mixtures as there are independent sources ($M \geq N$). In our research we considered $M = N$. We shall try to extract the desired EEG signal from the interference. The mixture is supposed to be linear and instantaneous, so that observations at time *t* instant result from a linear combination of the sources at that instant.

$$x_i(t) = \sum_{i=1}^{N} h_{ij} s_j(t) \qquad i = 1.....M.....(1)$$

Where h_{ij} are the unknown or the blind mixing coefficients that produce $x_i(t)$. For our research work we have modeled the system as $N \times M$ system and $N=M$. It may be a difficult for us to assume in the beginning that EEG data received for m electrodes is synthesized by exactly *N* statistically independent components as we ultimately can not know the exact number of independent components embedded in the EEG data. When the sources are in large number it is better to represent equations in Matrix forms as:

$$X = HS.....(2)$$

Where *X, H* and *S* can be represented in the following matrix forms.

$$X = \begin{bmatrix} x_1(t) \\ x_2(t) \\ \vdots \\ x_n(t) \end{bmatrix}; \quad S = \begin{bmatrix} s_1 \\ s_2 \\ \vdots \\ s_n \end{bmatrix}; \quad H = \begin{bmatrix} h_{11} & h_{12} & \cdots & h_{1n} \\ h_{21} & h_{22} & \cdots & h_{2n} \\ \vdots & & & \\ h_{n1} & h_{n2} & \cdots & h_{nn} \end{bmatrix} .....(3)$$

Suppose mixing parameters h_{ij} where $j=1\ldots\ldots n$, and the mixing is purely linear then this problem can be solved simply by inverting the mixing matrix *H*. But the Blind Source Separation means that we know nothing about h_{ij} $s_n(t)$. Hence the above equation(3) becomes more difficult. During EEG recording it is impossible to know how the signals were mixed with in the brain before they are picked up by the electrodes.

Independent Component Analysis (ICA) is a technique used to decompose a set of multivariate data in to underlying statistically independent components. Hyvarinen and Oja has rigorously defined ICA using statistical "latent variables" model[5]. Under this model *N* variables $x_1, x_2,\ldots\ldots x_n$ are observed. These variables are linear combinations of *N* latent variables $s_1, s_2\ldots\ldots,s_n$ as:

$$x_i = a_{i1}s + a_{i2}s_2 + ... + a_{in}s_n \quad for\ all\ i = 1,....,n \quad .....(4)$$

Where a_{ij}, $j=1,\ldots\ldots\ldots n$ are real coefficients. We have assumed that sources s_i are statistically independent. The source variables s_i are latent variables named as independent components. These variables are termed as "latent" because they can not be observed directly. Both the independent components, s_i and mixing coefficients a_{ij} are unknown and are required to be

determined or estimated after observing the data x_i. The best representation of ICA latent variables is in the form of Matrix. According to equation 2 where matrix H producing X can represent the original multivariate data as:

$$S = \left[s_1, s_2, s_3 \cdots s_n \right]^T \text{.....(5)}$$

According to equation(2) ICA tries to determine unmixing matrix W as per following equation

$$W \approx H^{-1} \text{.....(6)}$$

This gives the resulting matrix as:

$$Y = WX = W(HS) = S^{/} \approx S \quad (W \approx H^{-1}) \text{.....(7)}$$

3. THE ICA MODEL

There are m scalp electrodes of EEG picking up correlated brain signals. we are interested to know how effectively independent brain sources produce these signals. Our ICA model suited this scenario because it satisfies the most of the previously defined assumptions. We start with the assumption that collected EEG data can be modeled as collection of statistically independent brain signals. Assumption 2 is plausible and assumption 5 is valid because volume conduction in the brain is significantly instantaneous. We are interested to separate m observed EEG signals in to n statistically independent components for validity of assumption 3 and 4. Since we do not know the exact number of independent components embedded in the EEG signals, hence it is quite difficult to assume whether EEG data recorded from m electrodes is made up of exactly n-statistically independent components.

3.1 Ambiguities and Solution.

The solution will have always the following ambiguities.

1. Since both H and S are unknown. So a constant S can be cancelled by the same constant dividing H and vice versa.

$$X = (k)H\left(\frac{1}{K}\right)S = \left(\frac{1}{a}H\right)\left(\frac{a}{1}S\right) = \left(\frac{b}{1}H\right)\left(\frac{1}{b}s\right) \text{.....(8)}$$

To obtain the required result we fix the magnitude of the independent components by assuming that all of them have $E\{s_i^2\}=1$. However, this still not give us the solution when constant=-1. From here we conclude that that multiplying an independent component by -1 will have no impact on the validity of the solution. So we can flip any number of independent components and solution will still be valid.

2. The Independent components may have different order as the order of the original sources. For example, if $S=[s_1,s_2,s_3.\ldots.s_n]^T$. The final solution may be any permutation of $Y=[s_1,s_2.\ldots.s_n]$ gives the same previous ambiguity. Since both H and S are unknown we can insert a permutation matrix, P and P^{-1} in the solution without any further change.

$$Y = \left(WP^{-1}\right)\left(PX\right) \text{.....(9)}$$

Here PX is the observed signal in another order and WP^{-1} is new mixing matrix estimated my ICA.

3.2 Statistically Independency and Whitening

The first and the foremost assumption of ICA is that the original signals are statistically independent. Means that if $s_1,s_2,\ldots\ldots s_n$ are n random variables and there joint probability density function is equal to the product of their marginal probabilities then $s_1,s_2,\ldots\ldots s_n$ are defined as statistically independent.

$$\int (s_1, s_2, s_3, ..., s_n) = \int (s_1) \int (s_2) \int (s_3) ..... \int (s_n) \text{.....(10)}$$

The un-correlation is defined as

$$E\left\{s_1 s_2 s_3 .....s_N\right\} = E\left\{s_1\right\} E\left\{s_2\right\} E\left\{s_3\right\} .....E\left\{s_n\right\} \text{.....(11)}$$

In ICA this characteristics is weaker as compare to statistically independence but it does not always imply independence. This imply when $s_1,s_2,\ldots\ldots s_n$ are Gaussian random variables.

This is an important preprocessing step before sending data through ICA. No doubt that whitening is a weaker property than statistical independence but it is slightly stronger than un correlation. Which means that the covariance matrix of X equals the identity matrix I.

$$E\left\{XX^T\right\} = I \text{.....(12)}$$

In our research for mixed data we means to linearly transform it by multiplying it with matrix V such that we obtain the resulting matrix Z is white

$$Z = VX = V(HS) = H^{/}S \text{.....(13)}$$

This whitening gives an important result that new mixing matrix $H^{/}$ is orthogonal means and its inverse is equal to its transpose. When X Transformed in to Y by some transformation matrix then the density of the Y can be written in terms of the original variable X as follows.

$$p(Y) = \frac{p(X)}{\left|J_y(X)\right|} \text{.....(14)}$$

Where $J_Y(X)$ is the jacobian of Y with respect to X. When X and Y scalar valued functions x and y respectively then the above relation can be simplified as:

$$p(y) = \frac{p(x)}{\left|\frac{\partial y}{\partial x}\right|} \text{.....(15)}$$

However, ICA can not separate the mixed components when latent variables are Gaussian. But what if some of the independent components are Gaussian and some are non-Gaussian? ICA can separate all non-gaussian variables but the Gaussian components can not be separated from one another. That is why we have assumed in our second assumption that there must be only one Gaussian random variables in S.

The entropy of $H(x)$, if x is a continuous random variable with probability density function pdf $p(x)$ can be defined as[25].

$$H(x) \equiv -\int p(x) \log p(x) = -E\{\log[p(x)]\} \text{....(16)}$$

This definition also holds for multivariate data. Hence the entropy of $X=[x_1,x_2,x_3,\ldots\ldots x_n]^T$ is as:

$$H(X) = -E\{\log[P(X)]\} \text{.....(17)}$$

When entropy is a measure of randomness in a variable then mutual information are the measure of the reduction in entropy of X having Y available in that variable when $X=[x_1,x_2,x_3,\ldots\ldots x_n]^T$ is a set of multivariate data then it joint entropy $H(X)$ and self information $I(X)$ are related as:

$$I(X) = \sum_{i=1}^{n} H(x_i) - H(X) \text{.....(18)}$$

Which shows that self-information $I(X)$ is equal to the difference of the sum of all marginal entropies and the joint entropy $H(X)$? So if we maximize the joint entropy $H(X)$, it will minimize the mutual information $I(X)$. That is why Bell & Sejnowski[27] use this reasoning to derive the ICA algorithm. The same algorithm we have used in our research work. Hence the aim of obtaining statistical independence is to minimize the joint entropy $H(Y)$ of Y.

A modified ICA algorithm can be derived using Sejnowski algorithm by considering a scalar-valued function x with a Gaussian pdf $f_x(x)$ which passes through a transformation function $y=g(x)$ for producing the output of pdf $f_y(y)$. This is similar to the following matrix operation

$$Y = WX \text{.....(19)}$$

The transformation function y for EEG data wills be the logistic sigmoid as:

$$y = g(x) = \frac{1}{1+e^{-u}}, \quad u = wx + w_0 \text{.....(20)}$$

Where w is the weight also called slope of y. w_0 is the bias weight to align the high density part of the input with y. We know that an increase in the joint entropy of the output $H(y)$ means a decrease in the mutual information(as we discussed earlier). When we align the high density parts of pdf of x with the high sloping parts of $g(x)$, the entropy of the output is maximized. The function $g(x)$ is monotonically increasing hence the pdf of the output $f_y(y)$ can be written as a function of pdf of the input $f_x)x)$ as follows:

$$f_y(y) = \frac{f_x(x)}{\left|\frac{\partial y}{\partial x}\right|} \text{.....(21)}$$

And the entropy of the output can be given as shown in the equation(22).

$$H(y) = -E\{\ln f_y(y) = -\int_{-\infty}^{\infty} f_y(y) \ln f_y(y) dy \text{.....(22)}$$

From equation 22 and 21 by substitution we get

$$H(y) = E\left(\ln\left|\frac{\partial y}{\partial x}\right|\right) - E\{\ln f_x(x).....(23)$$

For statistical independence we have to maximize *H(Y)* of above equation. In right hand side function *x* is fixed so the only variable we can change is *y*. Or we can say the slope *w* of *y*. taking partial of *H(Y)* with respect to *w*. The second term in above equation does not depend upon *w* and therefore, can be ignored. So the change in slope, Δ*w*, needed for maximum change in entropy is:

$$\Delta w\,\alpha\,\frac{\partial H(y)}{\partial w}\frac{\partial}{\partial w}E\left(\ln\frac{\partial y}{\partial x}\right).....(24)$$

For computing the derivative we cannot compute the expectation so we make the stochastic gradient expectation and we obtained the following simplified equation as:

$$\Delta w\,\alpha\,\frac{\partial H(y)}{\partial w} = \frac{\partial}{\partial w}\left(\ln\left|\frac{\partial y}{\partial x}\right|\right) = \left(\frac{\partial y}{\partial x}\right)^{-1}\frac{\partial}{\partial w}\left(\frac{\partial y}{\partial x}\right).....(25)$$

This equation is the general form of weight change rule for any transformation function *y*. For the logistic sigmoid function we evaluate the equation as:

$$\frac{\partial y}{\partial x} = wy(1-y).....(26)$$

$$\frac{\partial}{\partial w}\left(\frac{\partial y}{\partial x}\right) = y(1-y)(1+wx(1-2y)).....(27)$$

To get the weight update rule for *y* logistic sigmoid function we substitute equations 26, 27 in to equation 25 we get.

$$\Delta w_0\ \alpha\ w^{-1} + (1-2y)x.....(28)$$

And the bias weight update can be written as:

$$\Delta w_0\ \alpha\ 1-2y.....(29)$$

The similar steps we can derive the following learning for the sigmoid function as:

$$\Delta W \infty \left[W^T\right]^{-1} + (1-2Y)X^T.....(30)$$

$$\Delta W_0 \infty 1-2Y.....(31)$$

Where *y*=Logistic sigmoid $y=1/1+e^{-u}$ *u*=W x Data+w_0

We assume that *W* is the weights matrix which is obtained after running the ICA algorithm. A topographical plot of an independent component shows the strong EEG activity. Artifacts correction simply means removing a selected independent component from the observed EEG data in the figure 1 below. Regions of high magnitude (red and blue) denote concentrated EEG activity.

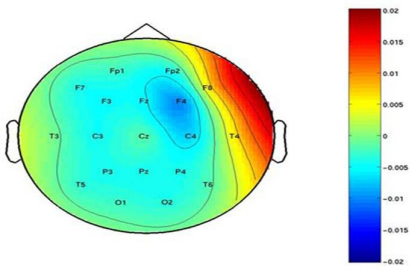

Figure 1. Topographic view of brain showing the intensity of EEG recordings. Maximum up red, minimum below blue

For observed EEG data *X*, the evaluated weight matrix *W*, the recorded EEG data is given by the following equation.

$$clean\_data = W_{inv}(:,a) \times ica(a,:).....(32)$$

Where

W_{inv}=Inverse of W
a=Vector of independent component
ica= Independent component obtained from *W*×*X*

FASTICA Flow Chart

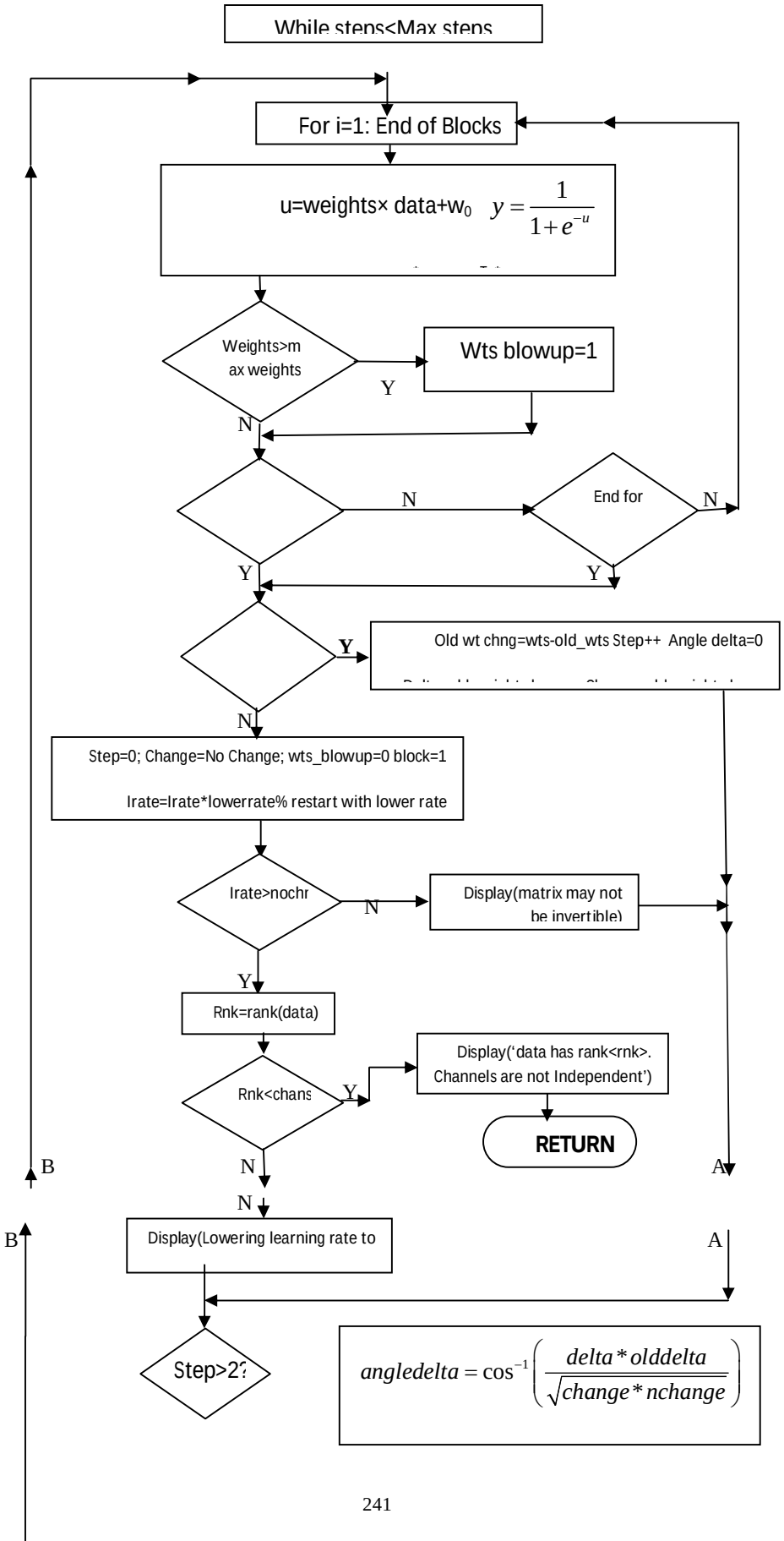

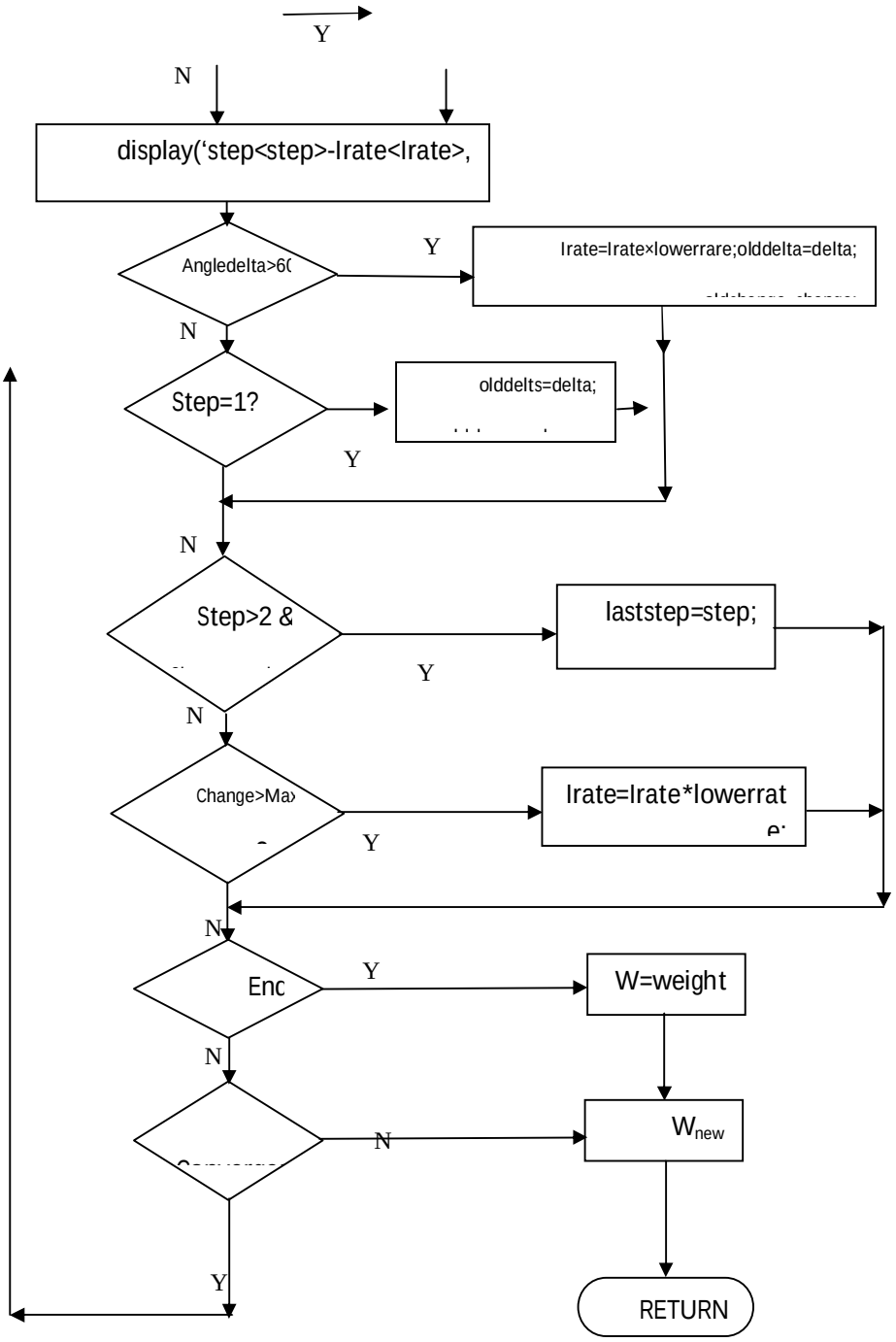

The following variables are used in the flowchart.

1. blocks=data is grouped in to blocks then processed.
2. Irate is the learning rate of algorithm
3. Lower rate=0.9 when the weights blowup
4. Max steps=512
5. angle delta=60 the rotation angle of probability function.
6. Irate is the learning rate of the of algorithm($1e^{-6}$).
7. lowerrate2=0.8 if change in ΔW>Max Wts.

3.3 The Algorithm FASTICA

The algorithm FASTICA contains the following steps

1) Zero mean the available mixed signal.
2) Make the data whiten.
3) Unit Norm the initial weight vector.
4) Consider

$$w_{new} = aE\{mg(w^T m)\} - aE\{mg'(w^T m)\}w \quad \text{……. ……(33)}$$

Here contrast function is represented by g.

5) Suppose

$$w_{new} = w_{new} / \| w_{new} \| \quad \text{…….} \quad (34)$$

Where w_{new} is representing weight vector. At every iteration it is updated.

6) Make comparison of old with new one, if there is convergence start another from new row, otherwise perform step 4.

$$\Delta \bar{w} = \bar{w}(n) - \bar{w}(n-1) \quad if \quad \|\Delta \bar{w}\| < \delta \text{ ……(35)}$$

Fast ICA is based on a fixed point iteration scheme for finding a maximum of the non-gaussianity of W^TX as measured in previous equations. This can also be obtained as an approximate Newton iteration denoted by g, which is the derivative of non-quadratic function g used in equation (33). The derivative of equations(34,35) are:

$$g_1(u) = \tanh(a_1 u), \quad g_2(u) = u \exp(-u^2/2) \quad (36)$$

Where $1 \le a_1 \le 2$. As suitable constant it is $a_1 = 1$. The basic steps for the FASTICA algorithm are following.

1. Choose an initial(random) weight vector
2. Let $W^+ = E\{Xg(W^T X)\} - E\{g'(W^T X)\}W$
3. Let $W = W^+ / \|W^+\|$
4. If not converged, go back to step 2.

It is important to note that convergence means that the new and the old values of W point in the same direction i.e their dot product is equal to 1. It is not necessary that the vector converges to a single point, since W and –W define the same direction. This is because the Independent components can be defined only up to a multiplicative sign. It is also assumed that the data is pre-whitened.

4 RESULTS AND DISCUSSIONS

In our work ICA is employed to eliminate EEG artifacts. The EEG signals have been used as vital source of clinical information for detection of brain and diagnoses of brain diseases. ICA algorithm adapted here is to differentiate ECG signals from tumor patients in to spatially orthogonal source signals. Moreover another statistically independent method is provided which automatically locate noise corrupted tumor related noisy ICA components. FASTICA is a most recently proposed method and it operate assuming availability of the scalp potential available in weighted sum. Considering this characteristic EOG, EEG and ECG signals can individually separate seeing in brain their independent sources.

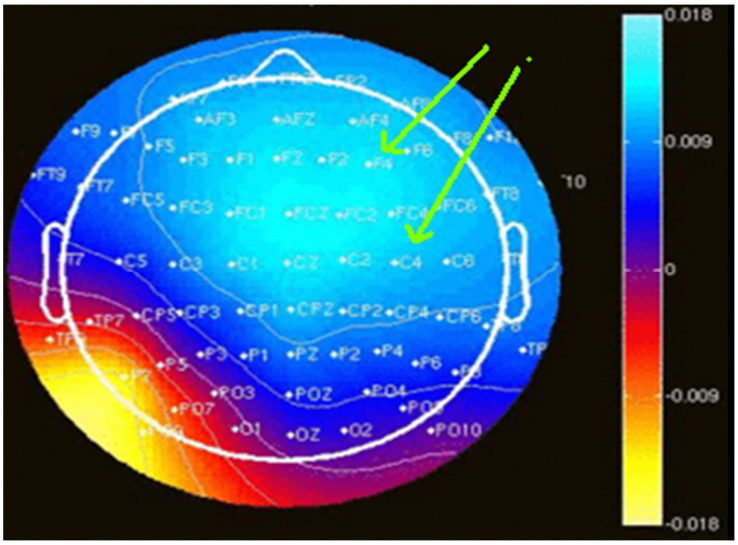

Figure 2. The scalp map of many ICA components

Figure 2. shows the scalp map of electrodes represents the ICA components which are compatible with their generation in separate domains. The synchronous coupling of neuronal activity occurs in a single brain area. Scalp map electrodes simply represent the projection of a single. These signals have equivalent dipole. The single or two-dipole components models have are amazingly with low residual scalp map variance this is best fitting. The projection obtained from such ICA components represents one or two symmetric patches of cortex. To resolve the problem we choose a BEM model as shown in figure 3 below..

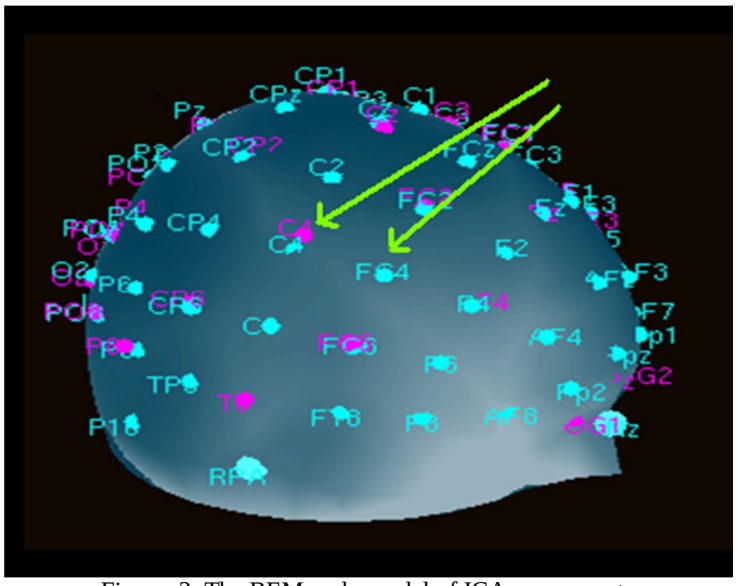

Figure 3. The BEM scalp model of ICA components

Selecting threshold on the maximum residual variance, the dipole location is not going to be assigned to those components which do not resemble dipolar field distribution. The electrode positions are projected t because of the dipole localization process and the respective skin surface of the BEM model as shown in figure 4 below.

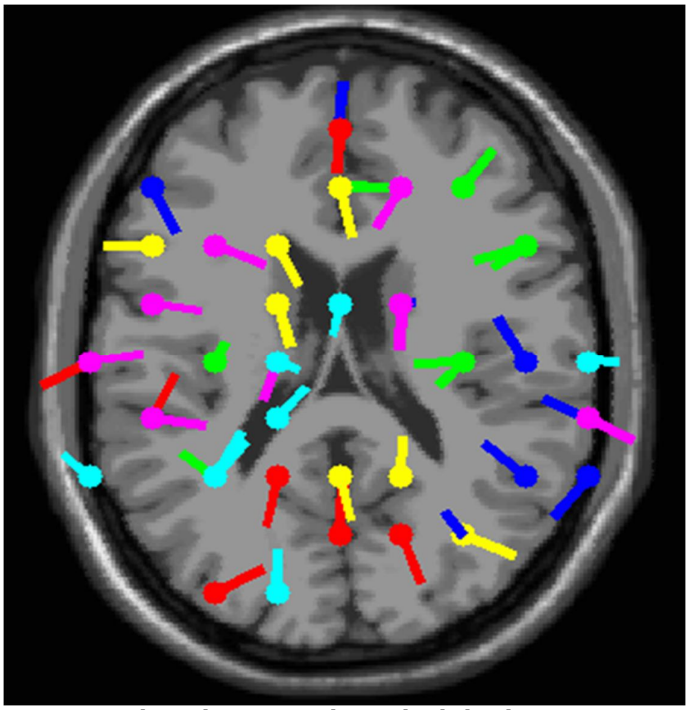

Figure 4 Electrode positions during dipole localization process

The electrode positions cannot be changed as are saved in the data se. All 3-D grid locations which are outside the head are excluded. At each remaining grid locations forward model (dipole to electrodes rejection) is computed and is compared with all component topographies. Figure above shows that all the dipoles has a residual variance is less than 40% vis a vis their component maps. It is notable that some components end up having the same x, y and z components. This happens because of the coarseness of the grid ERPs (Event related potentials) as shown by the brain response directly obtained from electrodes Figure 5 below.

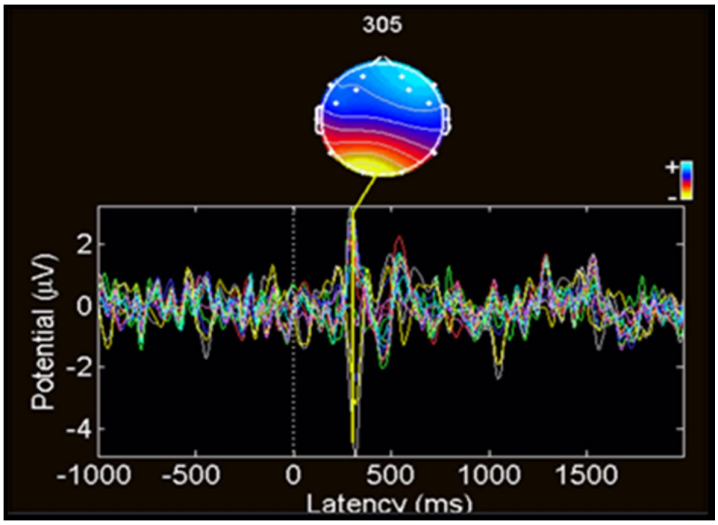

Figure 5 ERP waveforms of all channels

Figure 6 shows the appearance of ERP waveforms of all EEG channels and it shows that something has

happened at 305 milliseconds. From Figure 6 it is quite visible that channel 7 and channel 8(position of electrodes at C4& F4 at scalp electrodes 7 & 8 respectively) carries the highest ERP waveforms. Figure 7 showing the each single trial which is somewhat linear.

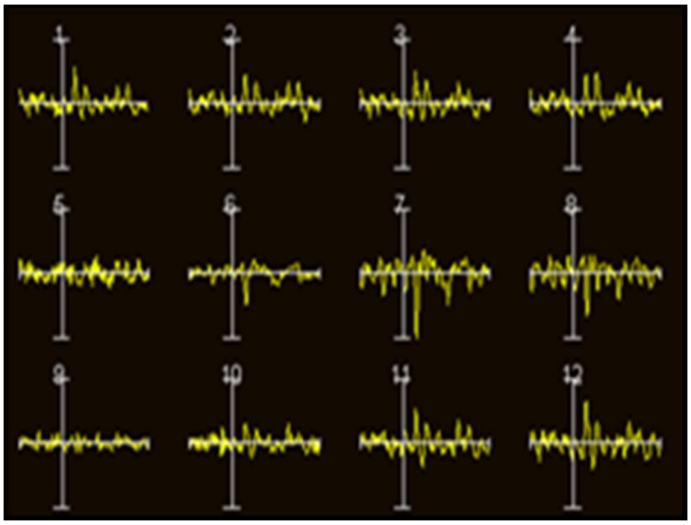

Figure 6. ERP waveforms of 12 channels for target events

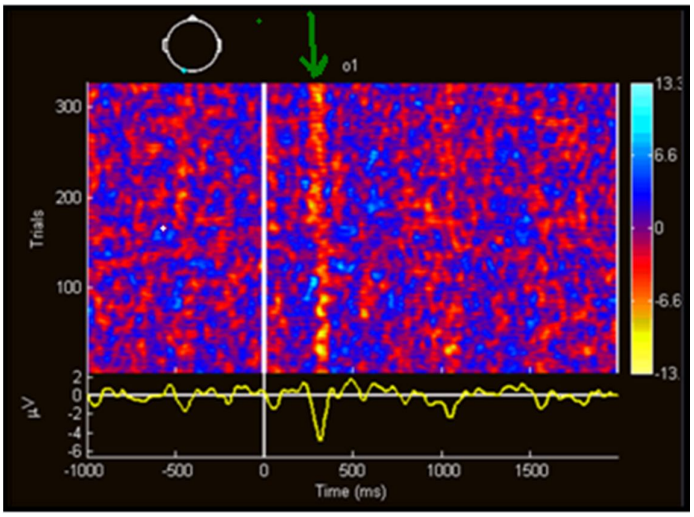

Figure 7. ERP waveforms for O1 and O2 for each single trial

4.1 Eliminating ECG artifacts from EEG

For eliminating ECG artifacts from EEG, the resultant data have also been analyzed with various signal to noise ratios and observed that the error standard deviation increases while decreasing signal to noise ratios. The breathing, movement of patient and movement of eyes are the main cause of baseline noise. Lose sensor contact, Eye and body movements. Different researchers have applied different techniques to remove this type of noise. These techniques are kalman filtering moving average and cubic spline. In this research we have applied independent component analysis (ICA) technique to remove the baseline wandering from electrocardiogram signals. The results are analyzed in terms of mean and standard deviation error signal. Figures 8 and figure 11 below shows two a typical EEG baseline noises signals observed at two different situations. Time in second (0-10000 m seconds) along x-axis and amplitude in voltages along y-axis shown in the figures below.

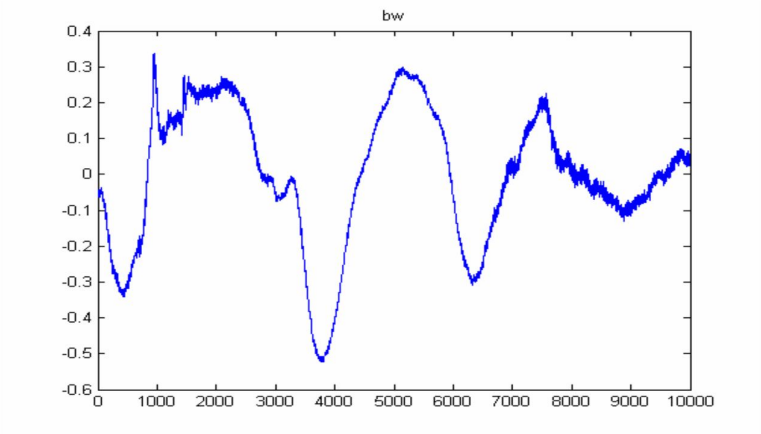

Figure 8. ECG Baseline Noise signal Case-I

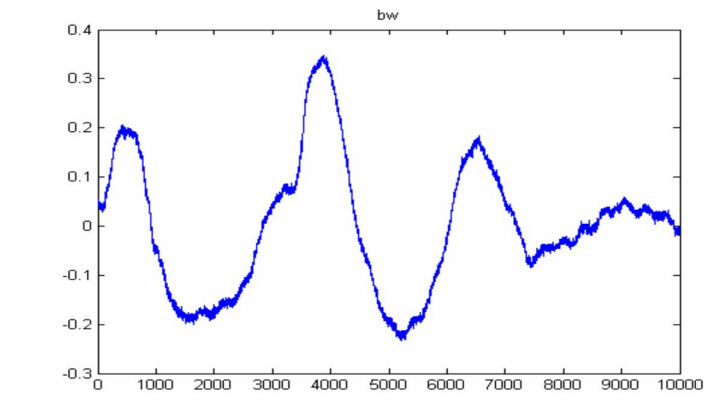

Figure 9. Another type of ECG Baseline Noise Signal Case-II

Linear combination of the input data which give independent components is obtained by Fast ICA. Figure 9 above shows the plot of input distorted data. This is a mixture of baseline wandering signal shown in figure 8 and the original ECG signal. Baseline wandering signal is a low frequency noise. It appears because of lose sensor contact, body movements and. Respiration. Then by using fast ICA algorithm un mixing matrix W was thus obtained. The resultant mixed signal as shown in Figure 10 is obtained by mixing the original ECG signal with baseline noise of figure 8.

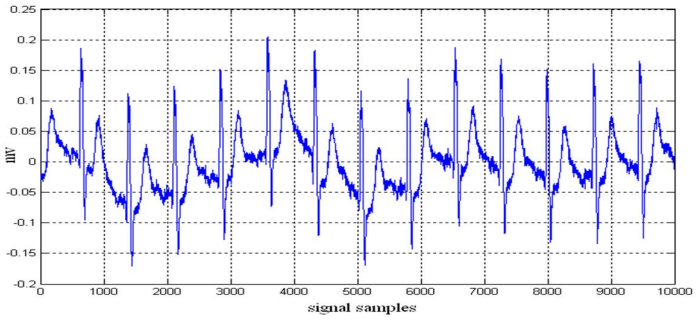

Figure 10. ECG Signal contaminated with baseline noise.

Figure 11 below shows the Gaussian noise when it is added with the original EEG signal, the resultant signal obtained is shown in the Figure 11 below.

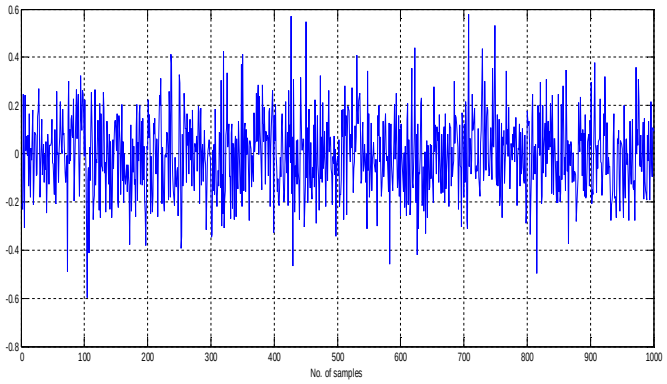

Figure 11. Resultant ECG Gaussian Noise mixed signal.

Figure 12 below shows the filtered ECG signal after application of ICA algorithm. This is a noise free signal and actual output of the ICA algorithm. Though the small amount of noise is still there however it can be easily eliminated from EEG signal.

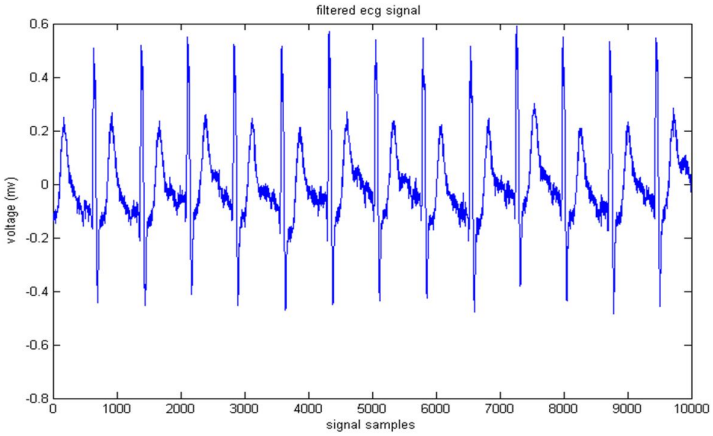

Figure 12. FASTICA applied Filtered ECG Signal

On the same grounds we again mix the noise signal as shown in figure 11 and fast ICA algorithm is applied. We obtain the signal as shown in figure 12 above. The results for both PPGA and ICA are summarized in the table1 and table 2.

Table 1. Results from figure 13

Algorithms	Mean Error	STD Error
Fast ICA	0.00039	0.0407
PPGA	1.0087e-004	0.0210

Table 2. Results from figure 14

Algorithms	Mean Error	STD Error
Fast ICA	0.0004724	0.045
PPGA	1.9667e-004	0.0323

For EOG artifacts the data set I shown in figure 13 contains 36 seconds of data with sampling frequency Fs=239Hz. There are 26 channels of data (19 channels shown). The data was collected from electrodes placed at the scalp on slandered locations using international system. As shown in the figure the data contains a seizure onset around t=299 which is evident on T3-T5 channels with the wavy waveforms. Muscles artifacts are appearing on all channels from t=304-315 shown on T4 & F8 channels. Occipital or rear head movement artifacts are appearing around t=280-385. Eye blink artifacts at Fp1,Fp2 are appearing around t=290-295. Compare this data with figure 13. Showing onset rhythmic wave on electrodes F4, C4 with dark blue area in figure 13.

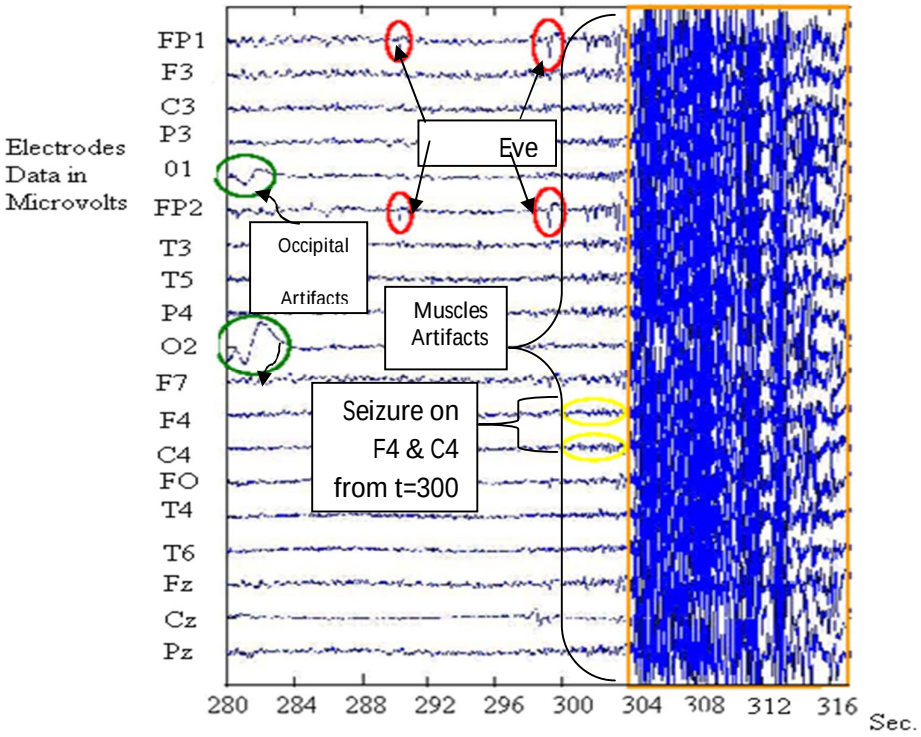

Figure 13. EEG Data from data set I

After running data through runica.m in EEG toolbox. The following resulting components shown in Figure 14 below are obtained. The artifacts shown in Figures 14 are eliminated using icapproj.m. The resulting EEG is shown in the figure below. It is evident that muscles artifacts have been reduced significantly.

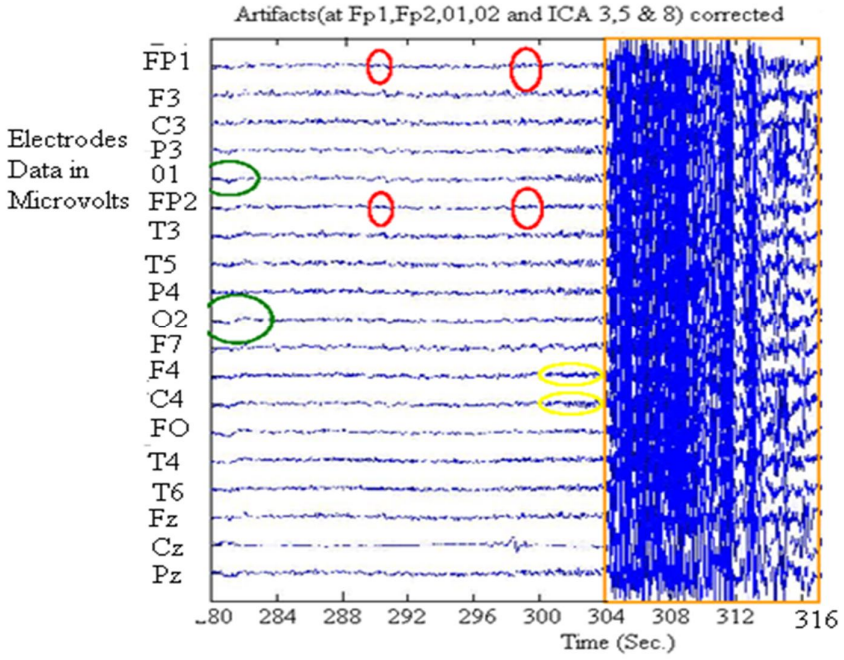

Figure 14. ICA artifacts eliminated

In data set I as shown in figure 16 above the muscle artifacts are not completely eliminated. In data set II below in Figure 15 we analyze the data from 1-90 second. The data is corrupted as shown in below.

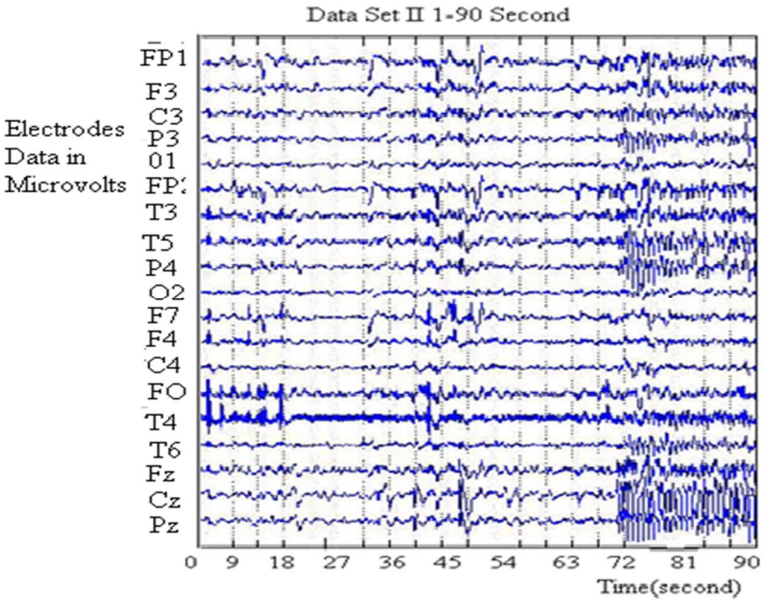

Figure 15. EEG corrupted data

Now we are able to detect the rhythmic waves showing the seizure in the brain. Here the ICA is successful in eliminating the muscles artifacts shown in figure 16 below.

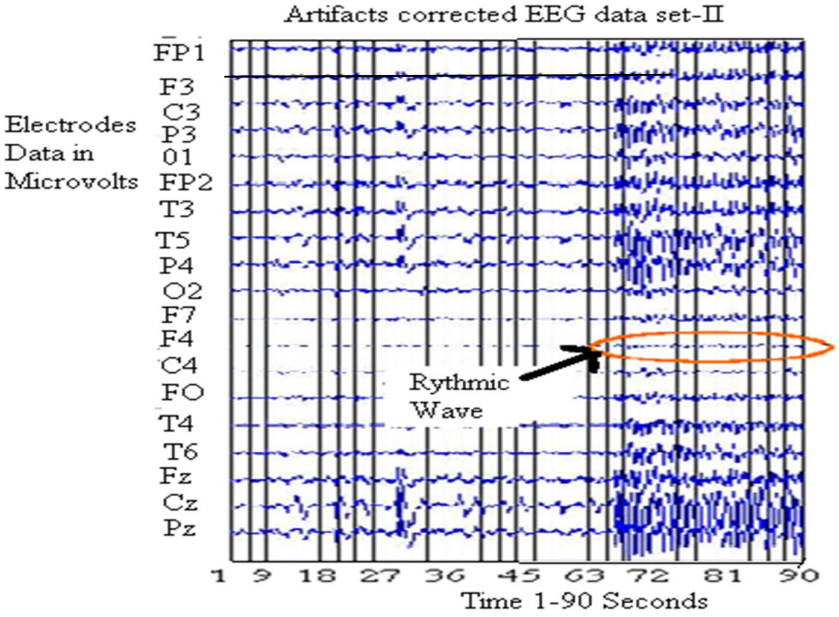

Figure 16 EEG Corrected data

Independent Component Analysis is a best technique used for elimination of artifacts on EEG data. One of the unique properties of ICA is that it can eliminate the artifacts alone without disturbing the surrounding EEG activity. Artifacts can also be eliminated simply by subtracting the frontal, temporal, and occipital readings from the EEG data. But this would lead to considerable loss in collected information. We have successfully eliminated eye and occipital artifacts from Data Set I and II. For Data set II shown in figures 15 and 16 respectively. FASTICA has also successfully revealed the rhythmic waves embedded in the artifacts just before the seizure onset at t = 90 sec. further amplified after passing through iris filter as shown in figure 17 below

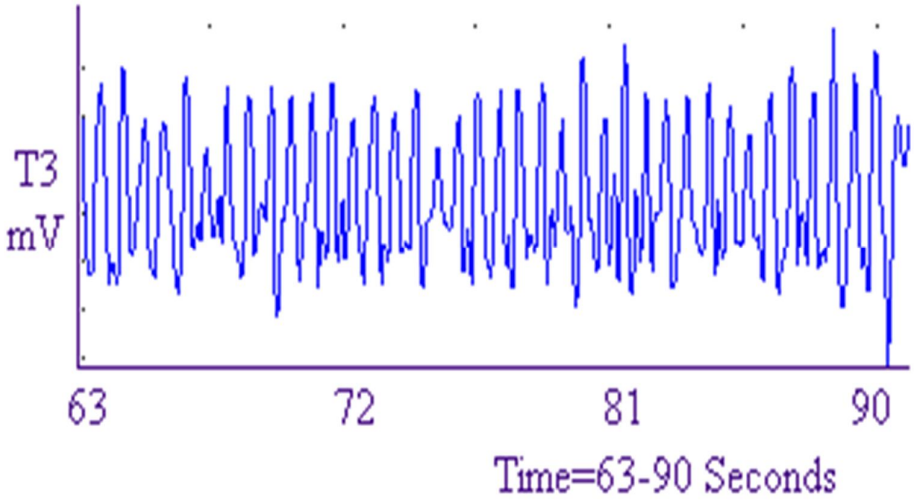

Figure 17. Rhythmic waves showing Seizure onset at t=90 sec

It is pretty much clear that the muscle artifacts appearing on all channels for Data Set I (t=305–315 sec) and Data Set II (at t=78-90, t=296-512, & t=582-592 sec) after a seizure onset are not removed or reduced significantly. We are unable to remove these artifacts significantly because these artifacts are not concentrated in any one region alone and hence the FASTICA algorithm cannot interpolate them as originating from any single electrode. Because of this reason it is difficult to get a single topographical or time plot of an independent component containing the muscle artifacts after a seizure onset. Moreover, since the person goes into severe spasms on the onset of the seizures, the muscle artifacts following it are of such large amplitude that they completely overshadow the EEG activity originating from within the brain.

Table 3. Signal To Noise Ratio for various EEG and Baseline Noise Signal

NO.	SNR	STD. Error	Mean Error
1	11	0.832	0.2172
2	22	0.613	0.4001
3	32	0.3158	0.3686
4	41	0.2931	0.3006
5	52	0.2203	0.2978

The EEG data of figures [14,91516,17] supported by the fMRI shows the brain activity more precisely. The fMRI results and EEG data results shows that the subject has left sided sensory Siezure as shown in Figure 18 below.

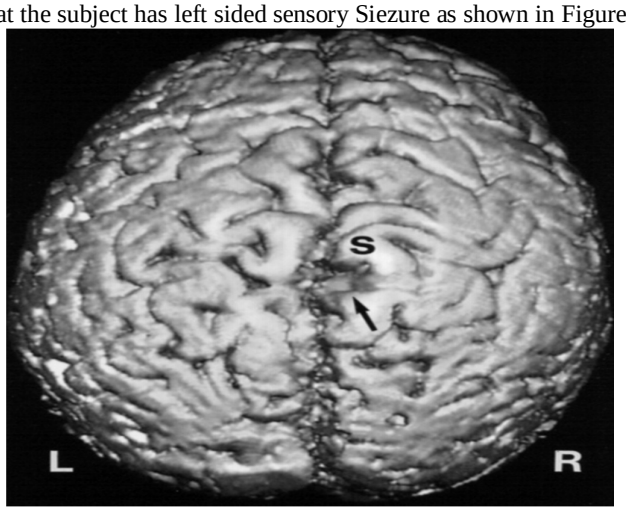

Figure 18. EEG results supported by fMRI Image.

Malignant tumors cell are more dense on boundaries. So clues for discriminating between malignant tumors and benign ones are believed to be mostly located in their boundary are as shown Figures [19, 20] below.

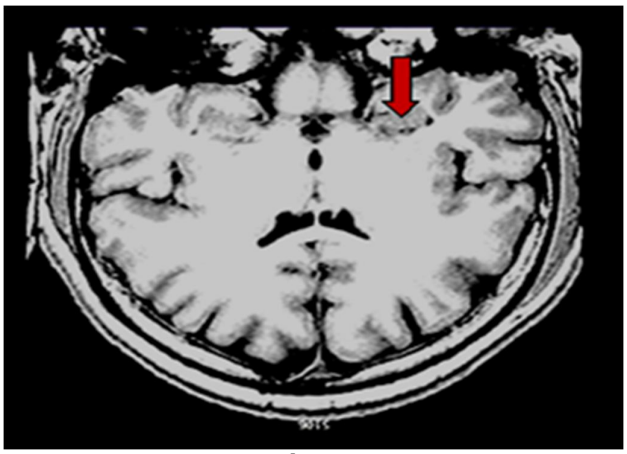

Figure 19. Malignant Tumor

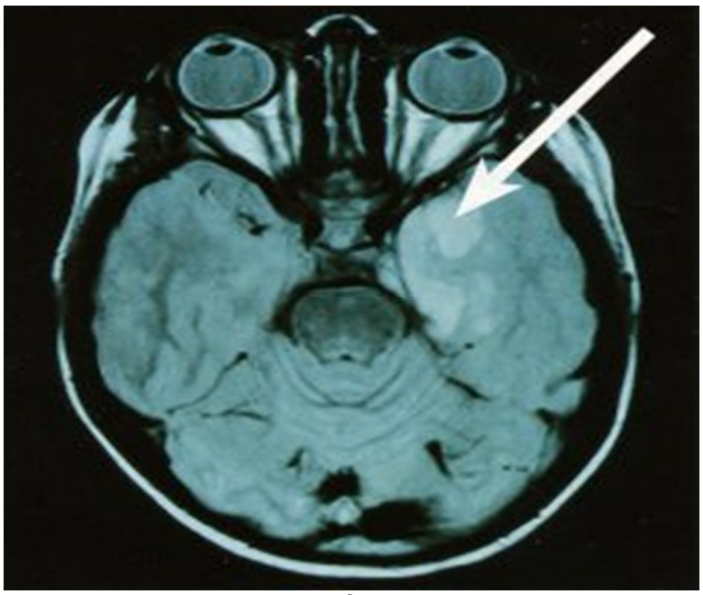

Figure 20 Malignant Tumor

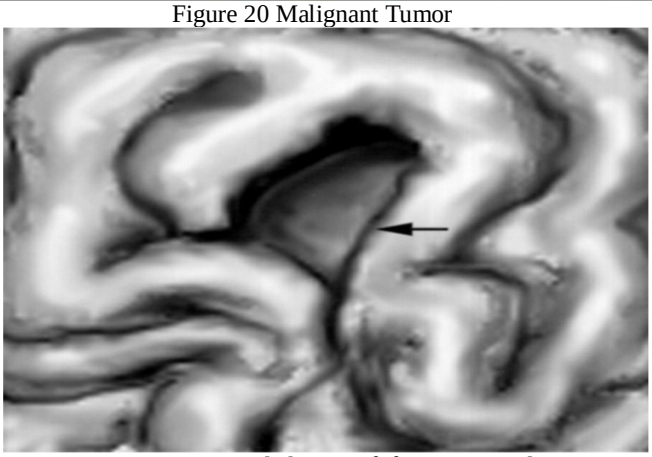

Figure 21. Expanded view of figures 19 and 20

The malignancy exhibit at times very weak contrasts to their background. The characterization of tumor candidates is necessary to identify malignant tumors. It is believed that important clues for malignancy are located around mass boundaries. Therefore, the detection of the boundary is an important preprocessing step as shown in Figure 22 below. .

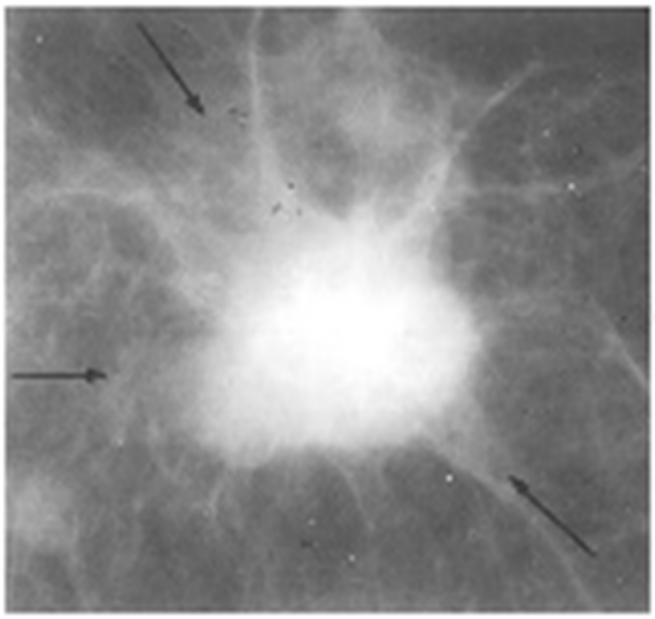

Figurw21.Malignancy a weak contrast to background

Malignant tumor has usually fuzzy boundaries. Because of the non-uniformity of the background, pixel values at the boundary of a particular tumor are not similar. Figure above shows the fMRI output. The shadow of a malignant tumor is visible at the lower left corner. We can see that the output for the tumor is very high and its region because of its fuzzy boundaries. Figure 22 below shows the EEG lab simulation of effected area.

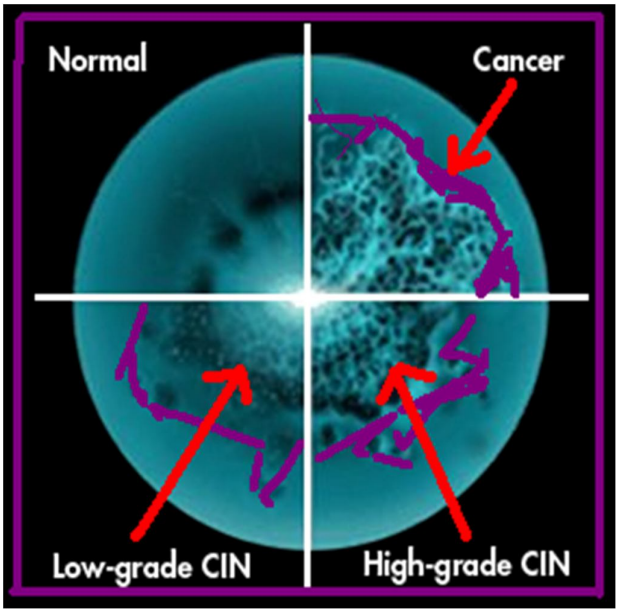

Figure 22. Tumor effected area as per ICA components

5. CONCLUSION

EEG is a basic tool used to measures brain activity. EEG IS widely used for brain tumor detection and other biomedical researches. This paper presents a system of efficient Malignant tumor detection involving a two-steps process. In the first step All artifacts effecting EEG signal have been eliminated successfully as a pre-diagnosis stage of malignant tumor. EEG signals are highly contaminated from subject, equipments and from many other electromagnetic sources. We have employed EEG simulation data set I,II. The noise corrupted signals are cleaned Employing FASTICA. In the second step the filtered clean EEG signals are then supported with the fMRI (functional magnetic resonance) for efficient Malignant brain tumor detection. fMRI provide detailed information about brain tumor.

Brain tumor are uncontrolled proliferations of cells. When the cells are originated from the brain itself Malignant tumor is called Primary tumor. When cell spread to brain from other locations of human body then tumors are termed as secondary. Primary Malignant brain tumor appear as hypo intense dark areas in fMRI T1 weighted images(figures 21,22 and 23) and hyper intense bright areas T2 weighted images figure 24. Blind source separation technique applied for removal of this noise is quite simple and converges in a few steps as compare to other adaptive filtering techniques and hence FASTICA employed EEG signals supported with the fMRI provide a system for efficient detection of malignant brain tumor.

Acknowledgment

The authors declare that they have no conflicts of interest in this research.

REFRENCES

1. Akram Rashid, Zahooruddin and Dr. I.M. Qureshi "Electrocardiogram Signal Processing for baseline Noise Removal using Blind Source Separation Techniques: A Comparative Analysis" IEEE Trans on Machine Learning and Cybernetics Guilin, Guangxi, China July 2011. Volume 4, pp1756
2. A.E.H. Emery, "Population frequencies of inherited neuromuscular disease-A world survey", *Neuromuscular Disorders*, Vol 1, No 1, pp. 19-29, 1991
3. Prabhakar K. Nayak and Niranjan U . Cholayya " Independent component analysis of Electrpencephalogram", *IEE Japan Papers of Technical Meeting on Medical and Biological Engineering* Vol.MBE-06, No.95-115,pp.25-28,2006.
4. Brain Tumor" from http://en.wikipedia.org/wiki/Braim tomor
5. H.G. Hosseini, H. Nazeran and K.J Reynolds, "ECG Noise Cancellation Using Digital Filters," *2nd International Conference on Bioelectromagnetism, Astralia, pp. 151-152, 1998.*
6. MA Mneimneh, Eeyaz, "An adaptive kalman filter for removing baseline wandering in ecg signal." *Computers in Cardiology, 2006;33:253–256.*
7. Steven Pacia, MD, "*Brain Tumors and Epilepsy"*, Fight against childhood epilepsy & seizures.
8. Dr. YW Fan, Dr. Gilberto KK Leung, " Management of seizure associated with brain tumor", *Medical Bulletin*, Vol. 11, No. 4, April 2006.
9. Aapo Hyvarinen, "A Family of Fixed-Point Algorithms for Independent Component Analysis," 0-8186-0/97 1997 IEEE.
10. Mangano FT, McBride AE, and Schneider SJ., "*Brain tumors and epilepsy"*, In: Ettinger AB and Devinsky O, eds. Managing epilepsy and co-existing disorders. Boston: Butterworth-Heinemann; pp. 175-194, 2002.
11. Aapo Hyvarinen "One-Unit Contrast Functions for Independent component analysis: A Statistical Analysis," Helsinki University of Technology, Laboratory of Computer and nformation Sciences, Finland.
12. Akram Rashid, Zahooruddin, Ijaz Mansoor Qureshi, Aamer Saleem "Electrocardiogram Signal Processing for Baseline Noise Removal USING Blind source separation techniques" International Conference on Machine Learning and Cybernetics, Vol. 4, pp 1756-1761, 2011.
13. Akram Rashid "Multiuser Detection in DS-CDMA using Evolutionary Techniques"International Conference on Computer, Electrical, System Science and Engineering, France Paris July 28-30. 2010.
14. C. Majos, M. Julia-Sape, J. Alonso, M. Serrallonga, C. Aguilera, J. Acebes, C. Arus and J. Gili, "Brain tumor classification by proton MR Spectroscopy: Comperison of Daignostic Accuracy at Short and Long TE", *American Journal Neuroradiology*, 25:1696-1704, November –December 2004.
15. Jie Li, Guan Han, Jing Wen and Xinbo Gao, "Robust tensor subspace learning for anomaly detection", *International Journal of Machine Learning and Cybernetics*, March 2011, DOI:10.1007/s1 3042-011-0017 -0.
16. Alfons Schuster and Yoko Yamaguchi, "From foundational issues in artificial intelligence to intelligent memristive nano-devices", *International Journal of Machine Learning and Cybernetics*, March 2011, DOI: 10.1007/s1 3042-011-0016 -1.
17. Weiguo Yi, Mingyu Lu and Zhi Liu, "Multi-valued attribute and multi-labeled data decision tree algorithm", *International Journal of Machine Learning and Cybernetics*, March 2011, DOI: 10.1007/s1 3042-011-0015 -2.
18. Jie Zhu, Xiaoping Li and Weiming Shen, "Effective genetic algorithm for resource-constrained project scheduling with limited preemptions", *International Journal of Machine Learning and Cybernetics*, March 2011. DOI: 10.1007/s1 3042-011-0014 -3.
19. Shumei Zhang, Paul McCullagh, Chris Nugent, Huiru Zheng and Matthias Baumgarten, "Optimal model selection for posture recognition in home-based healthcare", *International Journal of Machine Learning and Cybernetics*, Vol. 2, No. 1, pp. 1-14, 2011.

20. Yi Tang, Pingkun Yan, Yuan Yuan and Xuelong Li, "Single-image super-resolution via local learning", *International Journal of Machine Learning and Cybernetics*, Vol. 2, No. 1, pp. 15-23, 2011.
21. Fadi N Karameh, Munther A. Dahleh, "Automated classification of EEG/ECG signals in tumor diagnostic" , *Proceedings of American control conference,* Chicago, Illinois, June 2012.
22. R. Verleger, T, Gasser, & J. Mocks, "Correlation of EOG artifacts in eventrelated potentials of EEG: Aspects of reliability and validity" , *psychophysiology,* Vol. 9, pp 472-480,2011.
23. M. Murugesan, Mrs. R. Sukanesh " Towards Detection of Brain Tumor in Electroencephalogram Signals using Support Vector Machines", *International Journal of Computer Theory and Engineering,* Vol. 1 No.5, December 2011.
24. Shane M. Haas, Mark G. Frei, Ivan Osorio, Bozenna Pasik-Duncan, & Jeff Radel, "EEG ocular artifact removal through ARMAX model system identification using extended least squares", *Communication in Information and Systems* , 3,(1), pp 19-40, 2003.
25. M. Habl, Ch. Bauer, Ch. Ziegaus, E, W. Lang, F. Schulmeyer, " Can ICA help identify brain tumor related EEG signals?" *International Workshop on Independent Component Analysis and Blind signal Separation,* Helsinki, Finland, 19-22 June 2012.
26. Alexander V. KRAMARENKO, Uner Tan, "Effects of High Frequency Electromagnetic Fields : A Brain Mapping Study", *International Journal of Neuroscience,* Vol. 113, pp. 1007-1019, 3003.
27. Anthony J. Bell & Terrance J. Sejnowski, "AN information-Maximization approach to Blind separation and Blind deconvolution ", *Neural Computation* , Vol 7 pp,1004-1034, 2011.
28. Patange V.V & Deshmukh B.T "O.C.R.-A Method of Computes and Works on the Vision of Scanned Image" *International Journal of Electronics, Communication & Instrumentation Engineering Research and Development,* Vol. 2- 3, pp. 38-44, Sep. 30, 2012
29. Chumman Lal, Chandarkar et al, "Survey of Image Contrast Enhancement Methods*", International Journal of Electronics, Communication & Instrumentation Engineering Research and Development* , Vol. 2-3, pp. 56-63, Sep. 30, 2012.
30. Usha Rani at al, "Image Developing Techniques –A Comparative Study", *International Journal of Electronics, Communication & Instrumentation Engineering Research and Development,* Vol. 2-3,pp. 64-74, Sep. 30, 2012.
31. B.Srevanthi & C.H. Madhuri Devi, "Compressed Sensing Image Recovery Using Adaptive Nonlinear Filtering", *International Journal of Electronics, Communication & Instrumentation Engineering Research and Development,* Vol. 2-3, pp. 75-80, Sep.30, 2012.
32. AbhinavDeshpsnda & S.K.Tadse, "Design Approach For Content-Based Image Recovery using Gabor-Zemike Features", *International Journal of Electronics, Communication & Instrumentation Engineering Research and Development,* Vol.2-3 pp. 81-87, Sep. 30, 2012.
33. Ms. P. Swati Sowjanya & Ravi Mishra, " Video Shot Boundary Detection", *International Journal of Electronics, Communication & Instrumentation Engineering Research and Development,* Vol.1-2, pp.72-83, Dec. 2011.
34. N. R. Pal and S. K. Pal , "A review on image segmentation techniques," Pattern Recognition , vol. 26, no. 9, pp. 1277-1294, 1993[2]
35. L. P. Clarke, R. P. Velthuizen, M. A. Camacho, J. J. Heine, M.aidyanathan, L. O. Hall, R. W. Thatcher, and M. L. Silbiger, "MRI segmentation: methods and applications, Magn Reson Imaging , vol.13, no. 3, pp. 343-68, 1995.
36. M. B. Suchendra, K. B. Jean, and S. B. Minsoo , "Multiscale image segmentation using a hierarchical self-organizing map, Neurocomputing, vol. 14, pp. 241-272, 1997[4]
37. S. Murugavalli and V. Rajamani , "A high speed parallel fuzzy cmean algorithm for brain tumor segmentation, BIME Journal, vol. 6, 2006[5]
38. S. Murugavalli and V. Rajamani, "An improved implementation of brain tumor detection using segmentation based on neurouzzytechnique, J. Comp. Sc . vol. 3, no. 11, pp. 841-846, 2007.[6]
39. J. Chunyan, Z. Xinhua, H. Wanjun, and M. Christoph, "Segmentation and quantification of brain tumor, IEEE International Conference onVirtual Environment, Human-Computer Interfaces and Measurement Systems , USA, pp. 12-14, 2004.
40. L. Yuille, P. W. Hallinan, and D. S. Cohen, "Features extraction from faces using deformable templates, International Journal of Computer ,vol. 8, pp. 99-111, 1992.[8]
41. J.Tang, "A multi -direction GVF snake for the segmentation of skincancer images, " Pattern Recognition, vol. 42, no. 6, pp. 1172-1179,June 2009.
42. F. Zou, Y. Zheng, Z. Zhou, and K. Agyepong , "Gradient vector flowfield and mass region extraction in digital mammograms," International Symposium Computer-Based Medical Systems , pp. 41-43,June 2011.
43. H. Zhang and G. Li, Application in stomach epidermis tumorssegmentation by GVF snake model, International Seminar on Future BioMedical Information Engineering , pp. 453-456, 2010.[11]
44. M. Kass, A. Witkin, and D. Trezopoulos, "Snakes: Active contour models,", International Journal of Computer Vision, vol. 1, no. 4, pp.321-331, 2012.
45. T. F. Cootes and C. J. Taylor, "Active shape models -smart snakes, " in Proceedings of British Machine Vision Conference, pp. 266-275, 2011.
46. C. Xu and J. L. Prince, "Snakes, shapes and gradient vector flow, " IEEE Transaction on Image Processing , vol. 7, no. 3 pp.359-369,March 2010.
47. J. Canny, " A computational approach to edge detection, " IEEE Transactions on Pattern Analysis and Machine Intelligence, vol. 8, no.6, Nov. 2010.